

<Original Paper>

Planar Dynamics of the Electric Charged Particles

전기전하의 평면계 동특성

Soo Joon Kang* and Kisoan Park**

강 수 준 · 박 기 순

(Received March 12, 1999 : Accepted April 24, 1999)

Key Words : Electric Charged Particle(전기 전하 입자), Electric Charged Sphere(전도체로 표면이 도포된 소형구), Equilibrium Angle(정적 평형상태의 전하입자의 위치), Electrostatic Frequency (전하입자 운동 진동수), Grounded Chamber Effect(접지효과)

ABSTRACT

The fundamental dynamic properties of the planar electric charged particle are investigated experimentally. The experiment is conducted using electric charged spheres(4 table tennis balls with conductive surfaces) suspended by insulating strings to cancel the gravitational force. The measurements of the equilibrium angles and the natural frequencies of oscillation agree well with the analytical predictions with some error, respectively.

요 약

본 논문에서는 평면 계에서의 전기전하 입자의 기본적인 동특성을 간단한 모델을 이용하여 실험적으로 살펴보았다. 실험에서는 전기전하입자 모델로 4개의 소형구(전도체로 표면을 잘 도포한 탁구공)를 사용하였으며, 측정시 중력효과를 배제하기 위하여 잘 절연된 줄에 매달린 형태를 적용하였다. 실험으로 측정한 평형위치(각도)와 전하입자의 고유동수는 계산된 값과 상당히 근접함을 보인다.

1. Introduction

The limitation in modifying a structure's gross performance (mass, size, damping, stiffness, slewing, etc.) by tailing material properties (fiber reinforcement, braids, weaves, energy dissipating parts, etc.) has led to the demand for performance modifications by means of active

components (pneumatic /hydraulic actuators, piezoelectric sensors /actuators, imbedded fiberoptic sensors, motors, etc.⁽¹⁻⁶⁾).

The forces that modify material properties and hence performance are internal electrical forces representing bonds between molecules. Within this context, designing consists of judiciously arranging the molecules to yield the desired properties.

In contrast, the presence of external electrical forces produced by free surface electrons, i.e., surface charges, is generally regarded as a

* 정회원, 공군사관학교 기계공학과

** 공군전투발전단

liability and is suppressed by appropriate insulation and grounding techniques⁽⁷⁾.

The specific application is an electrostatic positioning instrument developed at the Jet Propulsion Laboratory⁽⁸⁾. In this research, the material is electrically charged and controlled by the electrostatic force produced by set of properly arranged electrodes.

Another specific applications related electrodynamic characteristics are studied^(1,2). These researches suggest that surface charges, when appropriately controlled, can be turned from a liability into an asset.

In this paper, the fixed charged electroscope experiment is conducted using electrically charged spheres suspended by insulating strings to cancel the gravitational forces. The measured equilibrium angles of the charged particles and the natural frequencies of oscillation are compared with analytical predictions.

2. Physical System Concept

Adopting a discrete particles approach, the planar electrodynamic system under the influence of electrostatic forces is modeled by lumping masses of charged particles connected by massless bars, each having length h_i and flexural rigidity EI_i as shown in Fig. 1. As shown, black dots represent inertially fixed particles, and white dots represent moving

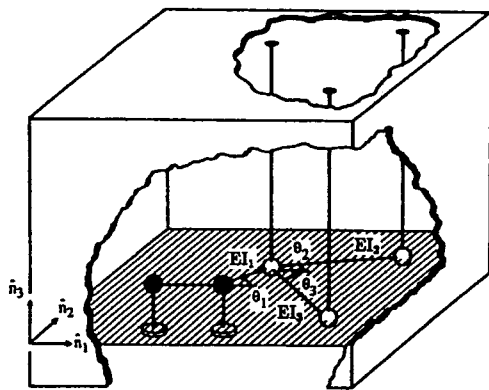


Fig. 1 Electrodynamic system

particles suspended by massless insulated strings. The motion is perpendicular to the gravity vector and is confined to the shaded $\hat{n}_1 - \hat{n}_2$ plane. θ_i denotes the i -th angular position relative to the \hat{n}_1 axis about the \hat{n}_3 axis. The system is enclosed in an electrically grounded chamber to minimize external electrical field disturbances and to minimize air current disturbances.

The forces acting on the particles are electrical forces, gravitational forces, elastic resorting forces and tension forces. The gravitational forces of attraction between particles are neglected.

3. Equations of Motion

The generalized coordinates, θ_j ($j=1,2,\dots, m$), make up a set of linearly independent displacements capable of describing an arbitrary configuration of the system. The position and velocity vectors of the particles, which are regarded as n point charges, are expressed as functions of m independent coordinates

$$\begin{aligned} \vec{r}_i &= \vec{r}_i(\theta_1, \theta_2, \dots, \theta_m) \\ \dot{\vec{r}}_i &= \sum_{j=1}^m \frac{\partial \vec{r}_i}{\partial \theta_j} \dot{\theta}_j, (i=1,2,\dots, n) \end{aligned} \tag{1}$$

in which $\vec{r}_i = x_i \hat{n}_1 + y_i \hat{n}_2$, ($i=1,2,\dots, n$) and θ_j ($j=1,2,\dots, m$) denote the position vector of the i -th point charge and the j -th angular position relative to the \hat{n}_1 axis about the \hat{n}_3 axis, and their overdots denote derivatives with respect to time, respectively.

The total potential energy of the electrodynamic system in Fig. 1 becomes

$$\begin{aligned} U &= \sum_{i=1}^{n-1} \sum_{j=i+1}^n \frac{x_i q_i q_j}{|\vec{r}_i - \vec{r}_j|} \\ &+ \frac{1}{2} \sum_{i=1}^m \sum_{j=1}^m k_{ij}^s \theta_i \theta_j \\ &+ \frac{1}{2} \sum_{i=1}^n \frac{m_i g}{L} |\vec{r}_i - \vec{r}_i^1|^2 \end{aligned} \tag{2}$$

in which $x_i, q_i, k_{ij}^s, m_i, g$ and L denotes

the electrical constant of the medium, i -th fixed electrical charges, mechanical stiffness matrix, mass of the i -th point charge, gravitational acceleration, and length of the insulated string, respectively. And in which $\vec{r}_i^1 = x_i^1 \hat{n}_1 + y_i^1 \hat{n}_2$ ($i=1,2,\dots,n$) denotes the nominal positions of the free ends of the suspending strings (The fixed end of the suspending strings are then located at $\vec{r}_i^1 + L \hat{n}_3$).

Invoking Lagrange's equations of motion for conservative systems and considering the relative angular positions $\eta_j(t) = \theta_j(t) - \theta_{j0}$, ($j = 1, 2, \dots, m$) and static equilibrium, now expressed in the functional forms

$$f_j(\eta_1, \eta_2, \dots, \eta_m, \dot{\eta}_1, \dot{\eta}_2, \dots, \dot{\eta}_m, \ddot{\eta}_1, \ddot{\eta}_2, \dots, \ddot{\eta}_m) = 0 \quad (j=1,2,\dots,m) \quad (3)$$

in which

$$f_j(0,0,\dots,0) = 0. \quad (j=1,2,\dots,m). \quad (4)$$

Taylor series expansions of Eq. (3) about a static equilibrium position yields a set of linearized equations of motion for the electrodynamic system.

$$\sum_{j=1}^m (m_{ij} \ddot{\eta}_j + k_{ij} \eta_j) = 0 \quad (i=1,2,\dots,m) \quad (5)$$

where

$$m_{ij} = m_{ji} = \left(\frac{\partial f_i}{\partial \theta_j} \right)_0 = \sum_{k=1}^n m_k \left(\frac{\partial \vec{r}_k}{\partial \theta_i} \right)_0 \cdot \left(\frac{\partial \vec{r}_k}{\partial \theta_j} \right)_0 \quad (6)$$

$$k_{ij} = k_{ji} = \left(\frac{\partial f_i}{\partial \theta_j} \right)_0 = \left(\frac{\partial^2 U}{\partial \theta_j \partial \theta_i} \right)_0 = \sum_{k=1}^{n-1} \sum_{l=k+1}^n \frac{x_k q_k q_l}{|\vec{r}_k - \vec{r}_l|^3} \cdot \left[2 \left(\frac{\partial |\vec{r}_k - \vec{r}_l|}{\partial \theta_i} \right)_0 \left(\frac{\partial |\vec{r}_k - \vec{r}_l|}{\partial \theta_j} \right)_0 \right]$$

$$- \sum_{k=1}^{n-1} \sum_{l=k+1}^n \frac{x_k q_k q_l}{|\vec{r}_k - \vec{r}_l|^3} \left(\frac{\partial^2 |\vec{r}_k - \vec{r}_l|}{\partial \theta_i^2} \right)_0 \delta_{ij} + \sum_{k=1}^n \frac{m_k g}{L} \left[\left(\frac{\partial |\vec{r}_k - \vec{r}_k^1|}{\partial \theta_j} \right)_0 \left(\frac{\partial |\vec{r}_k - \vec{r}_k^1|}{\partial \theta_i} \right)_0 + |\vec{r}_k - \vec{r}_k^1|_0 \left(\frac{\partial^2 |\vec{r}_k - \vec{r}_k^1|}{\partial \theta_j^2} \right)_0 \delta_{ij} \right] + k_{ij}^s, \quad (i, j = 1, 2, \dots, m) \quad (7)$$

where δ_{ij} is the Kronecker delta function. The associate set of m real modes of vibration are then governed by the eigenvalues problem

$$(\omega^{(k)})^2 \sum_{j=1}^m m_{ij} \phi_j^{(k)} = \sum_{j=1}^m k_{ij} \phi_j^{(k)}, \quad (i, k=1,2,\dots,m) \quad (8)$$

in which $\phi_j^{(k)}$ ($j=1,2,\dots,m$) denotes the k -th natural mode of vibration, and $\omega^{(k)}$ denotes the associated k -th natural frequency of oscillation. The natural modes of vibration are mutually orthogonal and can satisfy the orthonormality conditions

$$\phi_i^{(r)} m_{ij} \phi_j^{(s)} = \delta_{rs}, \quad \sum_{i=1}^m \sum_{j=1}^m \phi_i^{(r)} m_{ij} \phi_j^{(s)} = (\omega^{(r)})^2 \delta_{rs}, \quad (r, s=1,2,\dots,m). \quad (9)$$

4. Electrostatic Experiment

4.1 Experimental Setup

The electrostatic experiment is developed as an elementary two-degree-of-freedom electrodynamic system. The objective is to accurately measure the associated equilibrium angles and the electrostatic frequencies of oscillation. The electrostatic system consisted of four conductive spheres, a grounded plexiglass chamber and the measurement system shown in Fig. 2.

(1) The conductive spheres

The conductive spheres in this electroscope experiment are modeled as point charges as described in section 2. Each sphere, table tennis ball with the radius of 0.01883-m, is fabricated by a conductive material, Aquadag-E (it is supplied by Acheson Colloids Company, Port Huron, MI 48060). The properties and application method of Aquadag-E are given in Table 1 and 2, respectively.

The electrical characteristics of the dry coating can be varied by adjusting the ratio of

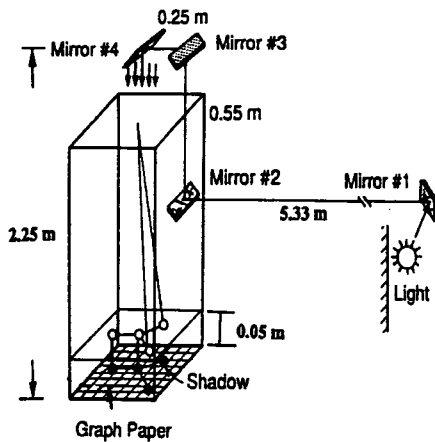


Fig. 2 Electroscope experimental and measurement system

Table 1 Properties of Aquadag-E

Pigment	Processed micrographite
Diluent	Deionized water
Color	Dark gray
Density	9.3 lbs/gal(1.12 kgs/1)
Freezing point	32F
Maximum service temperature	392F

Table 2 Application method of conductive material (Aquadag-E)

Method	Ratio	Thickness(dry)	Resistance
Dip	1:3	1.0 mil	30 ohms/sq
Spray	1:5	0.5 mil	150 ohms/sq
Brush	1:1	0.3 mil	1000 ohms/sq

* Ratio is grams of Aquadag-E to grams of water

concentrate to diluent, the method of application and thickness.

In this experiment, the brush method is used to coat ping pong balls with Aquadag-E. Fig. 3 shows the arrangement of the four conductive spheres enclosed in the grounded plexiglass chamber. As shown in Fig. 3, the q_1 , q_2 , q_3 and q_4 denote the charges of conductive spheres 1, 2, 3 and 4, respectively.

Two of them, q_1 and q_2 , are fixed in place at the bottom of the plexiglass chamber by a very thin insulated alumina rod. The other two, q_3 and q_4 , are suspended by the insulated strings from a common point directly above the central sphere q_2 , and are also pinned to the central sphere using rigid wire (gauge 28). The motion is perpendicular to the gravity vector thereby eliminating the gravitational and elastic effects.

The base of the plexiglass chamber has 7 small holes to change the position of q_1 . The length d is held constant (0.0635 m) and d_0 is the distance between the two fixed charges. The ratio d_0/d varies from 0.8 to 2.0.

(2) Grounded plexiglass chamber

The plexiglass chamber is 0.47 m × 0.73 m × 2.0 m and shielded with grounded aluminum wire screens. The safety measures built into the chamber consist of an interlock switch and a

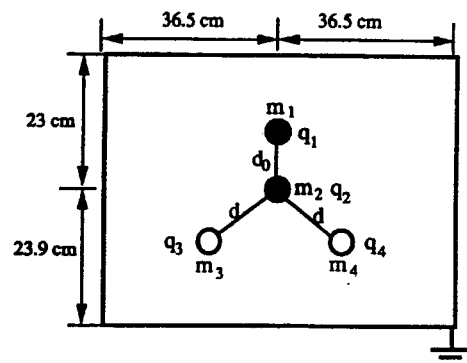


Fig. 3 Physical arrangement of the conductive spheres

limiting fuse as described in an inhouse operation manual⁽⁹⁾.

The electrically grounded chamber eliminates external electrical field disturbances and reduces air current disturbances.

(3) Measurement system

The measurement system consists of a far field light source (9.63 m) directed by means of four flat mirrors with the size of 0.2 m×0.2 m. The light casts shadows on the bottom of the chamber as shown in Fig. 2. Note that the use of multiple mirrors is required in order to sidetrack unavoidable obstructions that exist in the laboratory where the experiment is performed. In general, the generation of the far field light source does not require multiple mirrors. Indirect measurements of the positions of the spheres are obtained from the associated shadows created by high intensity light; a voltages of 120 V and a power of 600 Watts projecting lamp, directed downward from the top of the electrodynamic chamber. The bottom surface of the chamber is lined with 0.13 cm rectangular grid for equilibrium angle measurements and a two degree(2°) of the polar grid for natural frequency measurements. The position of the associated shadow can be measured with ±0.032 cm error and with ± 0.3° error. The measurements are video taped first and then evaluated.

4.2 Equilibrium

This experiment represents a two degree-of-freedom system where θ_1 and θ_2 are the angles of the charges q_3 and q_4 relative to the y axis as shown in Fig. 3. Computed equilibrium angles of the electroscope are compared with the measurements. The equilibrium angles are computed in two ways. The case of including image charges is considered first, and then the case of no image charges is treated.

(1) Grounded chamber effect

The effect of the grounded chamber is to introduce a null potential along the walls of

chamber in the plane of the motion of the spheres. Since the distances from each sphere to the walls of the grounded plane are much greater than the sphere radius (0.01883 m) shown in Fig. 3, each sphere's electric charge can be regarded as a point charge located at the center of the sphere. Based on the method of considering the image charges, the null potential is enforced by introducing massless image charges as shown in Fig. 4. For the number of angular displacement of charges, $m=2$, and the number of charged particles, $n=36$, and the magnitude of charges are related as follows:

$$\begin{aligned}
 q_{4k-3} &= (-1)^{k+1} q_1, \\
 q_{4k-2} &= (-1)^{k+1} q_2 \quad (k=1,2,\dots,9) \\
 q_{4k-1} &= (-1)^{k+1} q_3, \\
 q_{4k} &= (-1)^{k+1} q_4.
 \end{aligned}
 \tag{10}$$

Throughout the experiment $d=0.0635$ meters and $m_i = 2.7$ g ($i=1,2,3,4$). Only the nearest image charges as shown in Fig.4 need to be taken into account.

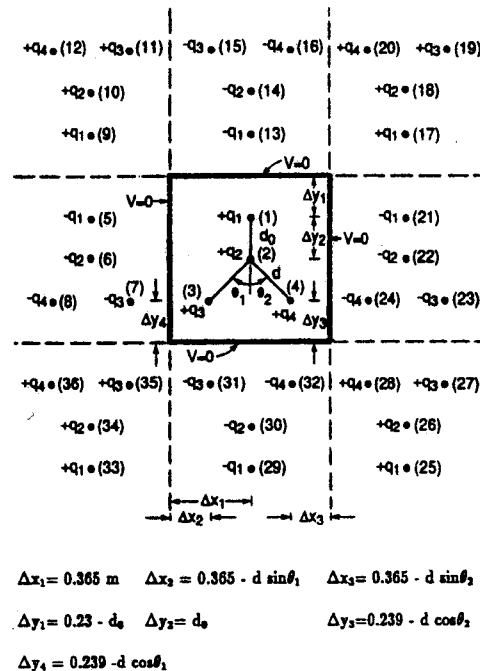


Fig. 4 Enforcement of null potential by means of image charges

(2) Computed charges

The charged spheres are electrically connected to a common power supply providing a regulated voltage of 20,000 V. In case of including image charges, the sphere charges q_i ($i=1,2,3,4$) can be obtained by potential $V=V_j$,

$$V_j = \sum_{i=1}^4 P_{ij} q_i \quad (j=1,2,3,4) \quad (11)$$

in which P_{ij} is the coefficients of potential, i.e.,

$$P_{ij} = \sum_{k=1}^4 \frac{x}{|\vec{r}_i - \vec{r}_k|}, \quad (12)$$

$(i, j=1,2,3,4; i \neq j)$

where \vec{r}_i denotes the position vector of the center of the i -th conductive sphere.

The coefficients of potential P_{ii} are given by⁽¹⁰⁾

$$P_{ii} = \frac{x}{r}, \quad (i=1,2,3,4) \quad (13)$$

in which r is the sphere radius. In the case in which image charges are included, the electrical potential of each sphere is given by

$$V_i = \sum_{j=1, i \neq j}^{36} \frac{x q_j}{|\vec{r}_i - \vec{r}_j|} + \frac{x q_i}{r}, \quad (14)$$

$(i=1,2,3,4)$

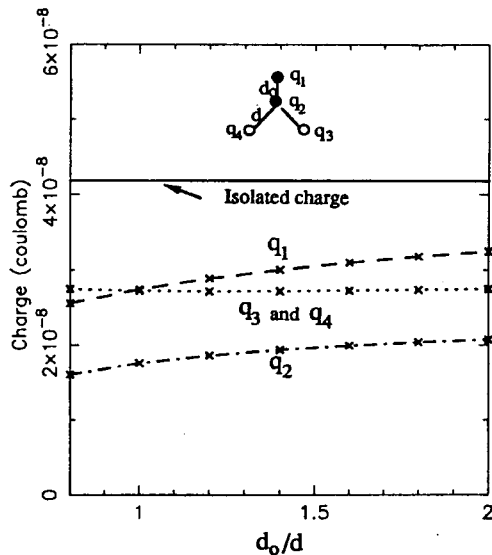


Fig. 5 Calculated charge of each sphere including images (All spheres charged to 20,000 V)

(3) Comparison of results

The gravitational effects and the elastic effects are eliminated in this experiment and in the calculations. Fig. 5 shows the computed charges of the conductive spheres at the static equilibrium position as a function of the length ratio.

The measurements of the positions of the spheres are obtained from the associated shadows as previously described. Fig. 6 shows a sample photograph of the equilibrium positions of the conductive spheres for a length ratio (d_0/d) = 1.2.

The measured equilibrium angle and the computed equilibrium angle are compared in Fig. 7. As shown, the differences between the measured and computed equilibrium angles are on the order of the resolution of the grid paper.

The effect of the grounded chamber is indicated in Table 3.

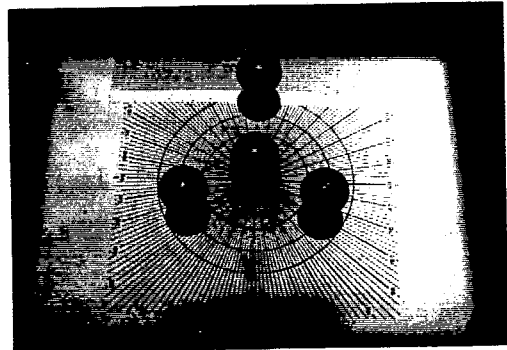


Fig. 6 Photograph of the equilibrium positions of the conductive spheres for a 1.2 length ratio

Table 3 Comparison of equilibrium angles (degree)

d_0/d	Measured	Calculated	
		No images	With images
0.8	57.25	59.89	57.67
1.0	57.75	60.00	57.91
1.2	58.60	60.69	58.74
1.4	59.90	61.74	59.93
1.6	61.10	62.91	61.34
1.8	62.90	64.19	62.92
2.0	64.50	65.51	64.63

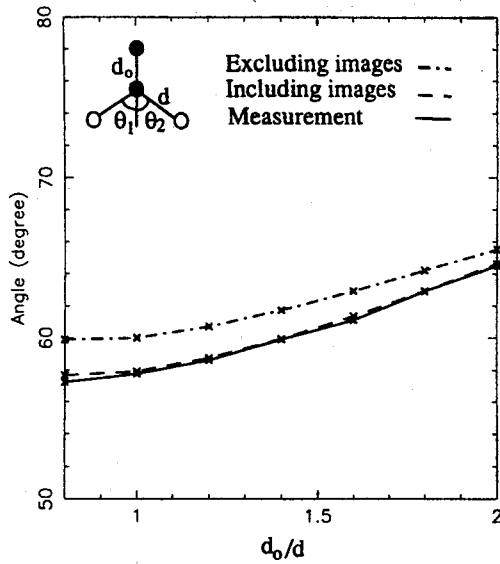


Fig. 7 Equilibrium angles versus length ratio (d_0/d)

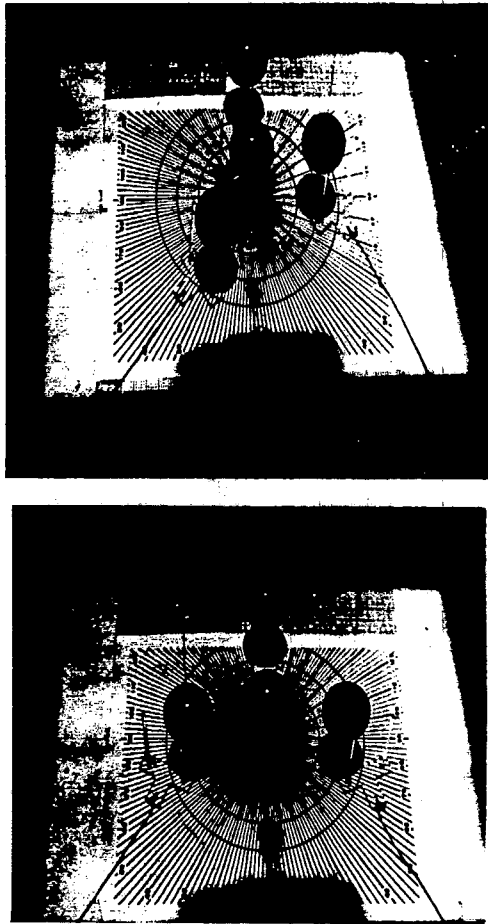


Fig. 8 Initial positions of the associated 1st mode (top) and 2nd mode (bottom)

Table 4 Comparison of electrostatic frequencies of oscillation (rad/sec)

d_0/d	Mode 1		Mode 2	
	Measured	Calculated	Measured	Calculated
0.8	1.121	1.285	2.004	2.049
1.0	1.102	1.270	1.973	2.377
1.2	1.070	1.222	1.865	2.319
1.4	1.024	1.169	1.838	2.248
1.6	0.976	1.101	1.744	2.170
1.8	0.942	1.029	1.697	2.089
2.0	0.903	0.951	1.668	2.009

4.3 Electrostatic Frequencies

The electroscope represents a two degree-of-freedom system that possesses two natural modes of oscillation and two associated electrostatic frequencies of oscillation. The first mode of oscillation, $(\theta_1, \theta_2) = (+1, -1)$, is associated with in-phase synchronous motion of the spheres. The second mode, $(\theta_1, \theta_2) = (+1, +1)$, is associated with out-of-phase synchronous motion of the spheres. Fig. 8 shows the initial positions of the associated modes.

The natural modes and the electrostatic frequencies can be computed from the

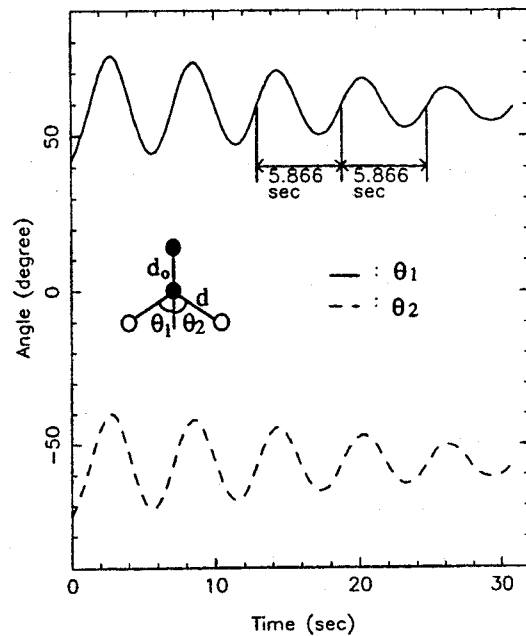


Fig. 9 Mode 1 response (damping factor=0.007, length ratio=1.2)

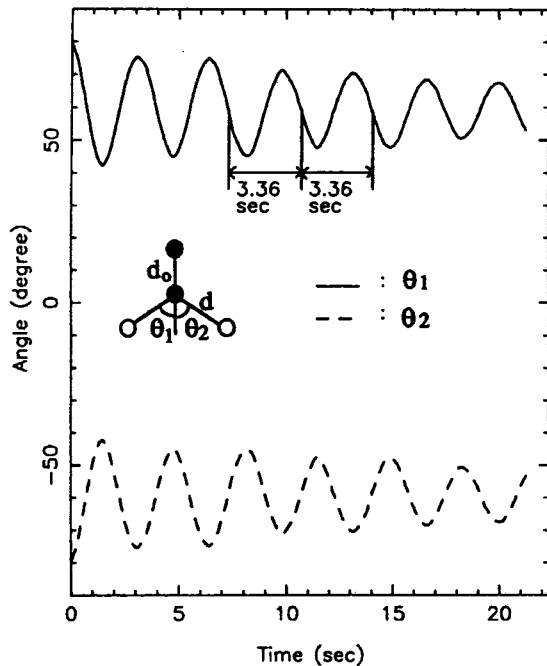


Fig. 10 Mode 2 response (damping factor =0.007, length ratio=1.2)

eigenvalues problem, Eq. (8), for the case of including image charges to see the effects of the grounded chamber. The measured natural frequencies and the computed natural frequencies are shown in Table 4.

Some error depicted in the results is attributed to the neglected non-linearity wherein the charges is assumed to be fixed in time for purposes of linearization. Typical single mode excitations are shown in Figs. 9 and 10.

6. Conclusions

The experiment is developed for studying dynamic systems whose motion is due only to isolated electrical forces. The resultant of all non-electrical forces is zero. The measured equilibrium angles agree well with the analytical predictions with an average error of 3%~0.19%. The measured natural frequencies of oscillation

also agree with the predicted values of natural frequencies with the 10%~20% error. The dominance of the linearity is attractive since under proper conditions it implies for electrodynamic systems having more complex geometries and for electrostatics with feedback control, that design strategies can readily be carried out on the basis of linear theories.

References

- (1) Park, Kisoan, 1992, "An Investigation of Planar Electrodynamic Structures", ph. D Dissertation, North Carolina State University, U. S. A.
- (2) Grohe, W., 1960, Precision Measurement and Gaging Techniques Chemical Publishing Co., NY.
- (3) Bryant, M. D. and Keltie, R. K., 1986, "A Characterization of the Linear and Nonlinear Dynamic Performance of a Practical Piezoelectric Actuator," Sensors and Actuator, Vol. 1.
- (4) Lewis, R., 1985, "Solid-State Cameras" Electronic Imaging, Vol. 4, No. 1.
- (5) Giachino, J. M., 1986, "SmartSensors," Sensors and Actuators, Vol. 10.
- (6) Kind, D. and Karner, H., 1985, High Voltage Insulation Technology, Friedr. Vieweg and Sohr Verlags-Gesellschaft, Braunschweig.
- (7) Rhim, W.K., Collener, M.T., Simms, W. T., and Elleman, D. D., 1985, "Development of an Electrostatic Positioner for Space Material Processing", Rev. Sci. Instrum. 56(2), pp. 307~316.
- (8) Doggett, W. O., and Silverberg, L., 1990, "Protective Chamber for Electrodynamic Experiments: Safety Measures and Operation Procedures", North Carolina State University, Internal Report.
- (9) Scott, W. T., 1966, The Physics of Electricity and Magnetism, John Wiley Sons Inc., NY.